COMPETITIVE REMOVAL OF MALACHITE GREEN AND RHODAMINE B USING CLINOPTILOLITE IN A TWO-DYE SYSTEM

Evrim Baran and Bilal Acemioğlu*

Department of Chemistry, Faculty of Science and Arts, University of Kilis 7 Aralik, Kilis 79000, Turkey

Abstract—Surface and groundwaters become contaminated with dyes due to discharge into the environment, which increases the risk of a number of human diseases. Many methods of dye removal from discharge waters at the source have been developed, but few are effective and the most effective method (activated carbon) is very expensive. The purpose of the present study was to test a natural zeolite (clinoptilolite type) as a potentially effective and inexpensive method to remediate dye discharge into the environment. In the removal experiments, malachite green (MG) and rhodamine B (RB) cationic dyes were used. The effects of various experimental conditions such as initial dye concentration, pH, and temperature on dye removal were investigated in a single-dye system. The degree of removal of MG and RB increased with increasing initial concentration and temperature of the dye in a single-dye system. An increase in pH decreased RB removal, but increased MG removal. In a two-dye system, MG and RB adsorption decreased by ~41.74 and 21.51%, respectively, due to competitive adsorption of the two dyes. Adsorption reflected a pseudo-second order kinetics model with high correlation coefficients ($r^2 = 0.996-1.000$) in single-dye and two-dye systems. Adsorption was most consistent with the Langmuir-1 and the Redlich-Peterson isotherm models with high correlation coefficients ($r^2 = 0.987-0.999$) in both systems. The Langmuir-1 adsorption capacities were determined as 43.86 and 44.25 mg/g for the removal of MG and RB in single-dye systems, respectively. In a two-dye system, the Langmuir-1 capacities were 20.62 and 31.54 mg/g for the removal of MG and RB, respectively.

Key Words—Adsorption Selectivity, Clinoptilolite, Malachite Green, Rhodamine B, Single- and Two-dye Systems.

INTRODUCTION

Many dyes have been produced for use in industries such as textiles, paper, cosmetics, rubber, and plastics. The total amount of these dyes produced internationally is $\sim 7 \times 10^5$ tons per year (Dawood and Sen, 2012). Dye pollution in the wastewaters of these industries creates significant environmental problems. If the dye-containing wastewaters are discharged to the environment, they may migrate into the surface and groundwaters. Human exposure to waste dyes may lead to diseases such as cancer and skin irritation. Such dyes should, therefore, be removed before the wastewaters are discharged into the environment. For this purpose, many methods such as coagulation, flocculation, chemical oxidation, electrochemical processes, osmosis, biological treatments, and adsorption have been developed to purify dye-containing wastewaters (Won *et al.*, 2008). Many of these methods, other than adsorption, give poor results. The advantages and disadvantages of each technique were reviewed by Dogan and Alkan (2003). Of these methods, adsorption by activated carbon is well known to be an effective method for the removal of organic, inorganic, and dye pollution from wastewaters. The large cost of activated carbon, however, restricts its application (Özdemir *et al.*,

2011). Many researchers have focused, therefore, on the use of low-cost adsorbents as an alternative to activated carbon. For example, many low-cost materials such as peat (Ho and McKay, 1998), fly ash (Acemioğlu, 2004), perlite (Dogan and Alkan, 2003), fungus (Acemioğlu *et al.*, 2010), bentonite (Özdemir and Keskin, 2009), sepiolite (Uğurlu, 2009), zeolite (Han *et al.*, 2010), cotton wastes (Ertaş *et. al.*, 2010), peanut shell (Samil *et al.* 2011), pine cone (Dawood and Sen, 2012), olive stone, and pirina (Uğurlu *et al.*, 2008; Öncel *et al.*, 2012) have been used as adsorbents to remove the unwanted dye pollution by adsorption. Natural zeolites consist of crystalline hydrated aluminum silicates with a framework structure containing pores occupied by water, alkali, and alkaline earth cations. Zeolites usually exhibit ion exchange and large adsorptive properties because they have a net negative structural charge (Alpat *et al.*, 2008). Various types of natural zeolites can be found: clinoptilolite, mordenite, phillipsite, chabazite, stilbite, analcime, and laumontite are just some examples. Offretite, paulingite, barrerite, and mazzite are much rarer (Wang and Peng, 2010). Clinoptilolite is one of the most abundant materials used internationally. The amount of clinoptilolite in Turkey is ~4.5 million tons (Sismanoglu *et al.*, 2010). In the present study, clinoptilolite was used as an adsorbent. Because zeolites have significant adsorptive properties, they are often preferred as adsorbents in the removal of metal ions (Alvares-Ayuso *et al.*, 2003; Sprynskyy *et al.*, 2006; Tarlan-Yel

* E-mail address of corresponding author:
acemioglu@kilis.edu.tr

and Önen, 2010; Tomic *et al.*, 2012) and dyes. In a single-dye system, many dye-adsorption studies have been performed using zeolite (Armagan *et al.*, 2004; Benkli *et al.*, 2005; Wang and Zhu, 2006; Alpat *et al.*, 2008; Vala and Tichagwa, 2013). The study of adsorption in multi-component systems is important because many industrial effluents contain a mixture of several dyes. For multi-component systems, few studies have been reported on the adsorption of dyes using clinoptilolite. For instance, the adsorption of reactive blue 21 and reactive red 195 onto clinoptilolite was studied by Sismanoglu *et al.* (2010). In a study by Hisarli *et al.* (2012), clinoptilolite was used as an adsorbent for basic blue 3 and basic blue 18 in single- and two-dye systems.

The competitive removal of MG and RB using clinoptilolite in a two-dye system has not been reported previously.

MATERIALS AND METHODS

Materials

Clinoptilolite (Cpt) was provided by the Enli Mining Company, İzmir, Turkey, and its characteristics are listed in Table 1. The cation exchange capacity (CEC) and particle size of the Cpt were determined using the same method as Ming and Dixon (1987) (Table 1). The MG and RB were purchased from Merck (Darmstadt, Germany) and were used without further purification (Table 2). The MG and RB have different ionization constant values, pKa. Malachite green is a weak acid and has two amino groups, giving the first pKa value as 6.9 and the second, due to the protonated amino group, as 10.3. Rhodamine B is a weakly basic dye, and has two amino groups and a carboxyl group. The pKa value for the deprotonated carboxyl group is 3.2, for the protonated amino group it is 4.2, and for the neutral form it is 11.5 (Table 2). The molecular sizes of MG and RB were determined to be 1.378 nm and 1.353 nm, respectively, according to the theoretical method described by Yazici *et al.* (2016).

Analytical techniques

A field emission scanning electron microscope (FE-SEM – Zeiss/Supra 55 SEM, Jena, Germany) equipped

with an energy dispersive X-ray spectroscopy (EDX) detector was used to study the morphological and surface characteristics of the Cpt. The SEM (EDS) measurements were performed at high vacuum and 10.00 kV EHT (electron high tension). A Fourier transform infrared (FTIR) spectrometer (FTIR RX-1, Perkin Elmer, Shelton, USA) was used to characterize the Cpt and examine the adsorption of MG and RB. An X-ray diffractometer (Rigaku RadB-DMAX II, Woodlands, Texas, USA) was used to study the crystal structure of the Cpt. The XRD analysis was performed using CuKα radiation at 40 kV and 40 mA between 0 and 80°2θ. A UV-Vis spectrophotometer (PG Instruments T80 UV-Vis spectrophotometer, Leicester, UK) was used to determine the concentrations of dyes. An ultrasonic cleaner was used to better dissolve the dye in preparing the high-concentration dye solutions (*i.e.* 100 mg/L) (Jeiotech UC-10 Ultrasonic cleaner, Lab companion, Seoul, South Korea).

Removal of dyes

The Cpt particles were sieved through a 100-mesh sieve (Retsch AS200, Haan, Germany), and the sieved samples were treated with 0.1 N HCl for 3−5 min to remove impurities. Then, the samples were washed well with distilled water and dried in an oven at 100ºC for 4 h before experiments.
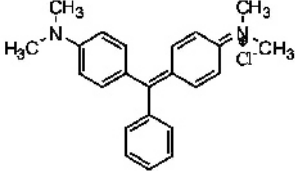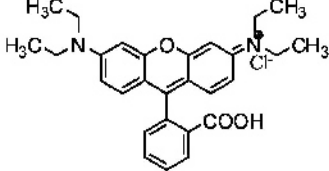
Removal of dye in a single-dye system

For a single-dye system, stock solutions of 1000 mg/L of the dyes were prepared. The desired concentrations were prepared by diluting the stock solutions. The experiments were performed by adding 0.05 g of the Cpt to 25 mL of dye solutions. The mixtures were then shaken in a temperature-controlled water bath. at various dye concentrations for up to 300 min: (20 mg/L (0.055 mM MG or 0.042 mM RB), 40 mg/L (0.110 mM MG or 0.084 mM RB), 60 mg/L (0.164 mM MG or 0.125 mM RB), 80 mg/L (0.219 mM MG or 0.167 mM RB), and 100 mg/L (0.274 mM MG or 0.208 mM RB)), pH values (3, 5, 7, or 9, adjusted with 0.1 M HCl or NaOH solutions), and temperatures (20, 30, 40, or 50ºC) for 5 h (*i.e.* equilibrium time). After shaking, each mixture was

Table 1. Clinoptilolite characteristics.

——— Chemical composition ———		———Physical properties———	
Compound	(wt.%)	Parameters	Value
SiO₂	67.11	Average pore radius (μm)	0.041
Al₂O₃	11.84	Porosity (%)	35.00
CaO	2.18	Surface area (m²/g)	40.79
Fe₂O₃	1.47	Density (g/cm³)	2.10
K₂O	3.44	CEC (meq/100 g)	55.14
MgO	1.15		
Na₂O	0.38		
Loss on ignition	12.50		

Table 2. Characteristics of MG and RB.

	Malachite green	Rhodamine B
Other names	Aniline green; Basic green 4; Diamond green B	Pigment Violet 1; Basic Violet 10
Chemical formula	$C_{23}H_{25}ClN_2$	$C_{28}H_{31}ClN_2O_3$
Molecular weight (g mol^{-1})	364.91	479.01
Solubility in water (25ºC) (g L^{-1})	40	50
Color According to pH (indicator function)	Below pH 2 — yellow pH 2−11.8 — green pH >13.8 — colorless	No indicator feature
λ_{max} (nm)	617	554
pKa	6.90[a], 10.3[b]	3.2[c], 4.2[d], 11.5[e]
Molecular structure		

[a] Maleki *et al.* (2012); Zou *et al.* (2014)
[b] Farhadi *et al.* (2010)
[c] Milanova *et al.* (2012)
[d] Zhang *et al.* (2011)
[e] George (1982)

centrifuged at $1992 \times g$ for 3 min to separate the solid particles from the liquid phase. In order to determine the concentrations of the dyes remaining in the solution, the supernatants were analyzed using a UV-Vis spectrophotometer at maximum absorbance wavelengths of the dyes (617 nm for MG and 554 nm for RB). A calibration curve was prepared by measuring the absorbance values of dye solutions at different concentrations over the range used in the experiments. The amount of dye removed per gram of adsorbent (q_t) and the removal efficiency (*RE*) of the dye at time *t* were calculated by equations 1 and 2, respectively.

$$q_t = \left(\frac{C_0 - C_t}{m}\right)V \qquad (1)$$

$$RE = \left(\frac{C_0 - C_t}{C_0}\right)100 \qquad (2)$$

where C_0 is the initial dye concentration (mg/L); C_t, the concentration of dye remaining in solution at any time (mg/L); q_t, the amount of dye removed per gram of adsorbent at any time (mg/g); *V*, the volume of the dye solution used (L); and *m*, the mass of adsorbent used (g). At equilibrium, q_t and C_t can be expressed as q_e and C_e, respectively.

Removal of dyes in a two-dye system

For a two-dye system, the experiments were performed for initial concentrations between 20 and 100 mg/L of MG at a constant initial concentration of 50 mg/L of RB using 500 mg/L stock solutions.

Similarly, the experiments were also done for initial concentrations between 20 and 100 mg/L of RB at a constant initial concentration of 50 mg/L of the MG. Assuming that no interaction occurs between the MG and RB, the total absorbance of the dye mixture in solution should be equal to the sum of the absorbance of each of the two dyes. The total absorbance is represented by equation 3. The concentration of each dye in a mixture was calculated using equations 4 and 5 (Chen *et al.*, 2011):

$$A_\lambda = A_{MG} + A_{RB} \qquad (3)$$

$$A_{\lambda 1} = \varepsilon_{1MG}bC_{MG} + \varepsilon_{1RB}bC_{RB} \qquad (4)$$

$$A_{\lambda 2} = \varepsilon_{2MG}bC_{MG} + \varepsilon_{2RB}bC_{RB} \qquad (5)$$

where A_{MG} and A_{RB} are the absorbance values of MG and RB at maximum wavelengths (λ_{max}), respectively; $A_{\lambda 1}$ and $A_{\lambda 2}$ are the total absorbance at wavelengths λ_1 and λ_2, respectively; ε_{1MG} and ε_{2MG} are the molar absorption coefficients of the MG at wavelengths λ_1 and λ_2, respectively; ε_{1RB} and ε_{2RB} are the molar absorption coefficients of RB at wavelengths λ_1 and λ_2, respectively; C_{MG} and C_{RB} are the concentrations of the MG and RB in the mixture, respectively; *b* is the path-length of the cell of 1 cm; and λ_1 and λ_2 are the wavelengths of maximum absorbance in the absorption spectra of the MG and RB, respectively.

For a two-dye system, the total removal efficiency (*TRE*) of the dyes was calculated using equation 6 (Yang *et al.*, 2011):

$$TRE = \left[\frac{\sum(C_{0,i} - C_{e,i})}{\sum C_{0,i}}\right]100 \qquad (6)$$

where $C_{0,i}$ and $C_{e,i}$ are the initial and equilibrium concentrations of the dye in solution (mg/L), respectively.

Adsorption isotherm

In order to study the adsorption isotherms, the equilibrium data were fitted to the Langmuir, Freundlich, Temkin, and Redlich-Peterson isotherm models (Langmuir, 1918; Freundlich, 1906; Temkin and Pyzhev, 1940; Redlich and Peterson, 1959) in single- and two-dye systems. The linearized equations of the isotherms can be written as shown below. In the present study, three linear types of the Langmuir isotherm were studied (Ofomaja and Ho, 2008):

$C_e/q_e = 1/Q_ob + C_e/Q_o$ Langmuir-1   (7)
$1/q_e = (1/Q_ob) 1/C_e + 1/Q_o$ Langmuir-2   (8)
$q_e/C_e = Q_ob - bq_e$ Langmuir-3   (9)
$\ln q_e = \ln k + 1/n \ln C_e$ Freundlich   (10)
$q_e = B \ln A_T + B \ln C_e$ Temkin   (11)
$\ln [K_R (C_e/q_e) - 1] = \ln (a_R) + \beta \ln (C_e)$
                     Redlich-Peterson   (12)

where q_e is the maximum amount of the dye removed by adsorbent at equilibrium time (mg/g); C_e, the equilibrium concentration of the dye in solution (mg/L); k and n, the Freundlich isotherm constants indicating the capacity and intensity of the adsorption, respectively; Q_o and b, the Langmuir isotherm constants indicating the capacity and the energy of the adsorption, respectively; B, a constant related to the heat of adsorption (J/mol), and is equal to RT/b_T, b_T is a Temkin isotherm constant; A_T, an equilibrium binding constant (L/g); T, the absolute temperature (K); R, the ideal gas constant (J/mol K); and K_R, a_R, and β, the constants of the Redlich-Peterson isotherm.

Adsorption kinetics

In order to study the adsorption kinetics, the experimental data were applied to kinetics models used by Lagergren (1898), Ho and McKay (1998), and Weber and Morris (1963). The linear forms of these models are expressed as follows:

$\text{Log } (q_e - q_t) = \log q_1 - (k_1/2.303)t$
   Pseudo first-order kinetics model, Lagergren (1898) (13)
$\frac{t}{q_t} = \frac{1}{k_2 q_2} + \frac{1}{q_e}t$ Pseudo second-order kinetics model,
            Ho and McKay (1998)   (14)

and

$q_t = k_i \cdot t^{1/2} + C$ Intra-particle diffusion model,
               Weber and Morris (1963)   (15)

where, t is contact time; q_e and q_t, the amounts of solute adsorbed per unit mass of adsorbent at equilibrium and

at any time, respectively; q_1 and q_2, theoretical adsorption capacities from the pseudo first- and second-order models, respectively; $k_2q_2^2$ indicates the initial adsorption rate; k_1 and k_2, the rate constants of the pseudo first- and second-order models, respectively; k_i, the rate constant of the intra-particle diffusion; and C, the intercept, indicating the thickness of the boundary layer between the adsorbent and the adsorbate.

RESULTS AND DISCUSSION

Characterization of Cpt

Analyses by SEM (Figure 1a) revealed that the Cpt surface was heterogeneous and rough, and was unchanged after dye adsorption (data not shown). Similarly, the crystallinity of Cpt, as revealed by XRD (Figure 1b), was unaffected by dye adsorption. Analysis by FTIR (Figure 1c), however, indicated that MG and RB were adsorbed on the cation exchange sites on the external surface of the Cpt because the particle sizes of the dyes were greater than that of the clinoptilolite. The EDS analysis of the Cpt suggested adsorption of MG and RB. The results of the FTIR and EDS analyses are explained in detail below. The dimensions of the 10- and 8-ring channels in Cpt were 0.44 nm × 0.72 nm and 0.41 nm × 0.47 nm, respectively, in agreement with Ming and Dixon (1987). Because the Cpt has small internal channels, the large dye molecules MG and RB cannot enter. These dyes, therefore, may migrate from the bulk phase to the cation exchange sites on the external surfaces of the Cpt.

Peaks in the XRD patterns were as expected at 9.8º, 11.16º, 16.86º, 17.24º, 22.32º, 26.06º, 28.06º, 30.06º, and 31.94º2θ, which correspond to Miller indices (*hkl*) of (020), (200), ($\bar{3}$11), (111), (131, 400), ($\bar{2}$22), ($\bar{4}$22), (151), and (530) corresponding to the crystalline planes of monoclinic Cpt.

FTIR analysis of the Cpt

The FTIR spectra of the Cpt were recorded over the wavenumber range $4000-650$ cm^{-1} using an attenuated total reflectance (ATR, Perkin Elmer FTIR-00-0251, Shelton, Connecticut, USA) spectrometer (Figure 1c). The weak peak observed at 3396 cm^{-1} indicates the vibration of OH...O bands in the structure of the Cpt (Hisarli *et al.*, 2012). After adsorption of the dyes, this band remained almost unchanged. The band at 1628 cm^{-1} probably indicates a deformation vibration of adsorbed H$_2$O (Hisarli *et al.*, 2012). After adsorption of the MG and RB, this band shifted to 1619 cm^{-1} and 1620 cm^{-1} in single- and two-dye systems, respectively. Also, very weak new peaks formed around 1585 and 1590 cm^{-1} after adsorption in single- and two-dye systems. In the case of MG and RB adsorption, new weak peaks were also observed at 1370 and 1339 cm^{-1}, respectively. These peaks may indicate a chemical activation resulting from an interaction between posi-
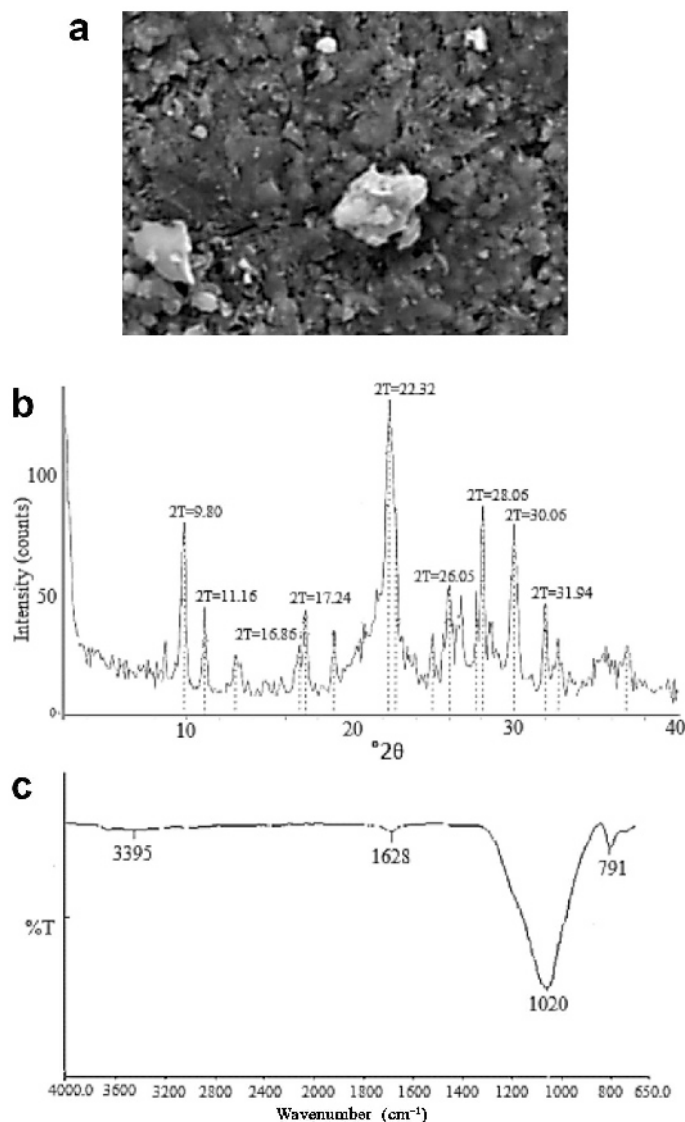
Figure 1. (a) SEM image, (b) XRD pattern (CuKα radiation), and (c) FTIR spectrum of Cpt.

tively charged nitrogen in the dye molecules and negatively charged oxygen in the Cpt. The very prominent band at 1020 cm^{-1} is assigned to Si−O(Si) stretching in the vibrations of the tetrahedral sheet (Farmer, 1974; Hisarli *et al*., 2012; Hernandez-Montoya *et al*., 2013). After adsorption of MG in a single-dye system, this band shifted to 1013 and the intensity increased. After the adsorption of RB in a single-dye system, this band shifted to 1015 cm^{-1} and the intensity decreased slightly. In the case of adsorption in a two-dye system, this band shifted to 1012 cm^{-1} and the intensity increased. The peaks at 792 and 726 cm^{-1} indicate the bending vibration of Mg−OH in the structure of the Cpt (Farmer, 1974, Uğurlu, 2009). After the adsorption of dyes in single- and two-dye systems, these bands shifted very slightly and the intensities increased slightly. All

these findings suggest that the Cpt has permanently charged cation exchange sites and has adsorbed the positively charged dyes.

EDS analysis of the Cpt

Analyses of the Cpt by EDS were performed before and after adsorption (Table 3a−d). The amounts of C and N on the Cpt increased after adsorption. These increases probably reflect the adsorption of organic dye molecules MG and RB on the external surface of the Cpt.

UV-Vis spectrophotometric analysis of MG and RB

In single- and two-dye systems, UV-Vis absorption spectra of MG and RB were recorded over wavelengths of 450 and 700 nm (Figure 2a,b). The maximum absorbance wavelengths of MG and RB were 617 and 554 nm,

Table 3. Energy dispersive spectroscopy results.

Element	(wt.%)	(at.%)
(a) Clinoptilolite		
O	45.24	57.48
Si	42.65	30.87
Al	4.65	3.50
C	3.15	5.33
K	2.80	1.46
Ca	0.69	0.35
N	0.55	0.79
Mg	0.20	0.22
(b) MG on clinoptioloite (single-dye system).		
O	45.16	54.38
Si	39.30	26.95
C	8.21	13.17
Al	4.16	2.97
K	1.16	0.57
N	1.01	1.39
Ca	0.72	0.35
Mg	0.26	0.21
(c) RB on clinoptilolite (single-dye system).		
O	49.03	59.38
Si	34.87	24.06
Al	5.84	4.19
C	5.64	9.10
K	1.96	0.97
Ca	1.24	0.60
N	0.96	1.32
Mg	0.40	0.38
(d) MG and RB on clinoptilolite (two-dye system).		
Si	48.35	35.24
O	26.41	33.78
C	12.59	21.45
Al	7.50	5.69
K	1.89	0.99
Ca	1.64	0.84
N	1.04	1.53
Mg	0.58	0.49

respectively. In a two-dye system, the absorption spectra were recorded for adsorption periods of between 1 and 300 min. The shapes and maxima of the absorption spectra of both dyes remained unchanged with adsorption time. The intensities of the absorption spectra of MG and RB in solution decreased with increasing contact times (Figure 2b), however, which indicated the reduction in the amount of dye in the medium.

Effects of experimental parameters on the removal of dyes in single-dye systems

The experimental conditions noted during the removal of MG and RB by the Cpt were contact time, initial dye concentration, pH, and temperature. The experiments were performed using an adsorbent dose of 2 g/L for a contact time of 5 h.

Effect of contact time and determination of equilibrium time

The effect of contact time on the removal of MG and RB by the Cpt was studied at different contact times of between 1.0 and 300 min under all experimental conditions: concentration, pH, and temperature. In single-dye systems, removal of MG and RB by the Cpt occurred within 15 min under all experimental conditions and, after 25 min, the amounts removed increased slowly until equilibrium was reached at ~15−90 min for low concentrations (20−60 mg/L) and at ~240−300 min for high concentrations (80−100 mg/L). Similar results were also reported for the adsorption of MG onto oil palm trunk fiber (Hameed and El-Khaiary, 2008a) and for the sorption of remazol brilliant blue R onto polyurethane-type foam prepared from peanut shell (Bilir *et al.*, 2013). The rapid removal of the dyes within the first 15 min was presumably due to the abundance of cation exchange sites on the surface of the Cpt. A similar result was reported for the adsorption of brilliant green dye on kaolin (Nandi *et al.*, 2009).
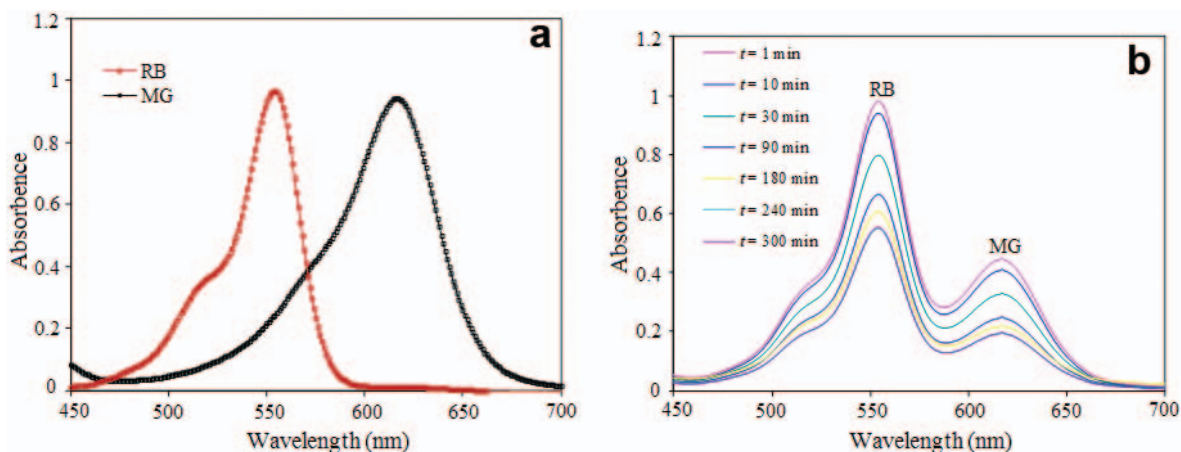

Figure 2. Molecular absorption spectra of MG and RB in a single-dye system (a) and in a two-dye system (b) as a function of adsorption time at 20ºC and natural pH.
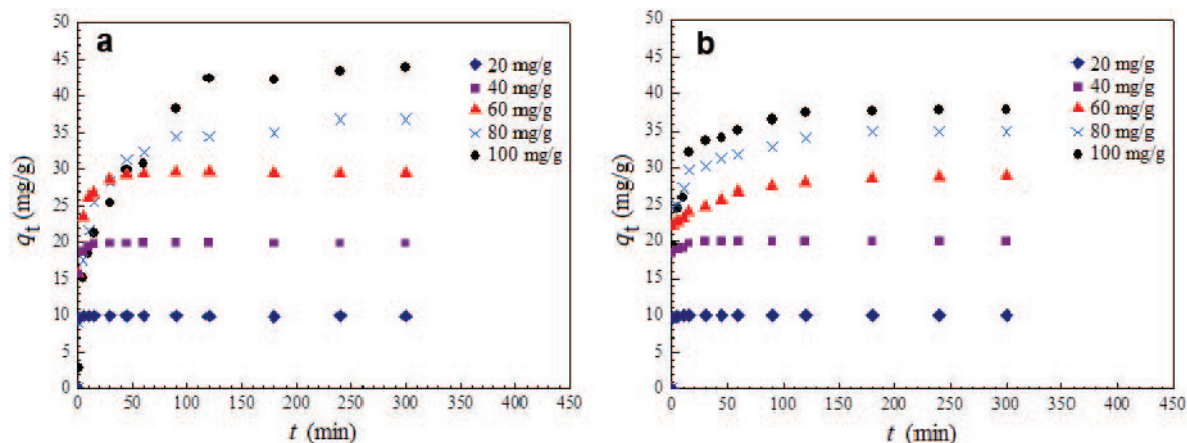
Figure 3. Effect of the initial dye concentration on the adsorption of MG (a) and RB (b) dyes onto Cpt in a 2 g/L suspension at 20ºC and natural pH.

Effect of initial dye concentration

The effect of the initial dye concentration on the removal of MG and RB by the Cpt was studied at natural dye pH (pH 4.12 for the MG and 4.18 for the RB) and 20ºC (Figure 3a,b). When the initial concentrations of MG and RB were increased from 20 to 100 mg/L, the amounts of MG and RB removed increased from 9.92 to 37.89 mg/g and from 10.0 to 37.74 mg/g, respectively. The fact that the adsorption of dyes increased with increasing initial dye concentration indicates that more adsorbent particles interact with more dye molecules. When the initial dye concentration was increased from 20 to 100 mg/L, the removal efficiencies of MG and RB decreased from 100 to 87.97% and from 100 to 72.15%, respectively. A similar trend was reported for the adsorption of MG onto chemically modified rice husk (Chowdhury *et al*., 2011).

Effect of pH

The pH of the medium in an adsorption process affects both the surface of an adsorbent and the ionization of a dye molecule. In these experiments, the effect of initial pH on the adsorption was studied for pH values between 3 and 7 for the MG and between 3 and 9 for the RB for an initial dye concentration of 80 mg/L at 20ºC. The results showed that the removal of the MG increased while the amount of the RB removed decreased with increasing pH (Figure 4a,b). A graphic showing the maximum removal of dye species as a function of pH, on the other hand, is shown for comparison (Figure 5). The cause of the increase in MG removal with increasing pH is attributed to the surface of the adsorbent having a more negative charge in the higher-pH medium. With increasing pH, an increase in the concentration of OH^- ions in solution occurs; these OH^- ions are adsorbed onto the surface of the zeolitic particles and the zeolite surface becomes more negative (Margeta *et al*., 2013). Dye removal, therefore, was increased *via* electrostatic interactions between more negatively charged Cpt and positively charged MG molecules (Figure 4a). Similar results were reported for the adsorption of MG onto rice straw-
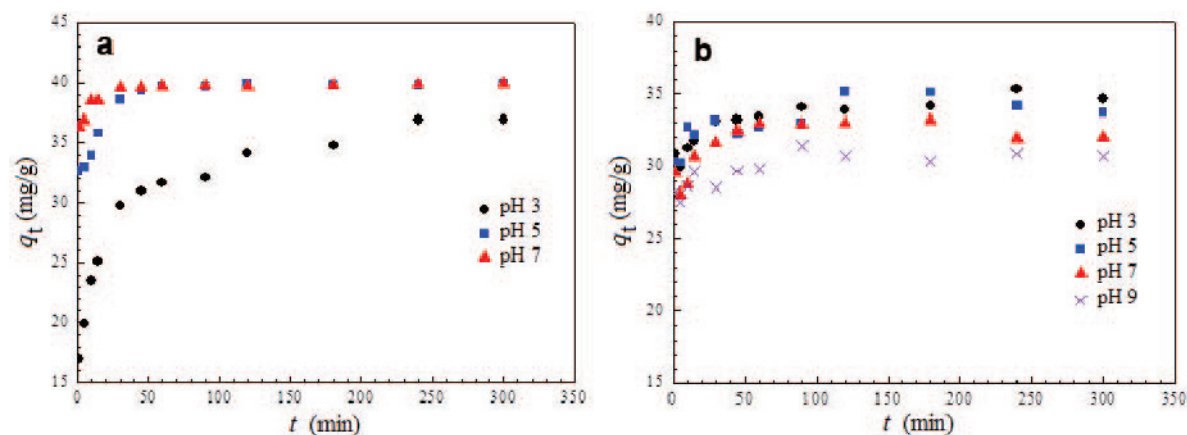

Figure 4. Effect of pH on the adsorption of MG (a) and RB (b) dyes onto Cpt in a 2 g/L suspension at 20ºC and 80 mg/L initial dye concentration.
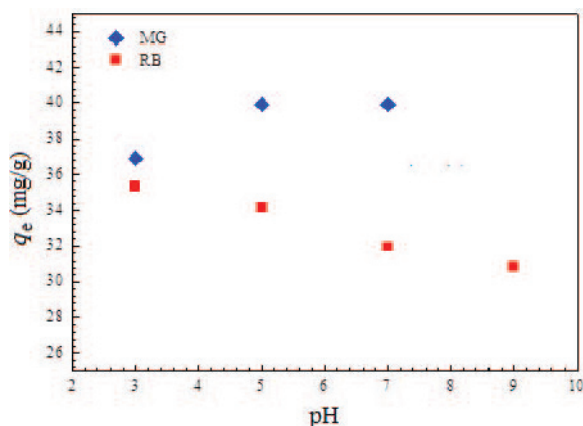
Figure 5. Comparison of the adsorption of MG and RB dyes onto Cpt in a 2 g/L suspension at 20ºC and 80 mg/L initial dye concentration as a function of pH.

derived char (Hameed and El-Khaiary, 2008b) and onto chemically modified rice husk (Chowdhury *et al.*, 2011). While more removal of RB should be expected at higher pH values, the removal of dye decreased with increasing pH. A similar result was also reported for adsorption of RB onto alumina-doped MCM-41 (Mobil Composition of Matter No. 41) (*i.e.* AlMCM-41) (Eftekhari *et al.*, 2010). The reason may be that the RB molecule occurs in a monomeric form at pH 3, and therefore the dye molecules may enter easily into the pores of the adsorbent (Guo *et al.*, 2005). At pH values of >3, the zwitterionic form of RB in water might cause the aggregation of the RB molecules and the aggregating dye molecules may not enter into the pores of the adsorbent (Anandkumar and Mandal, 2011).

Effect of temperature

The effect of temperature on the removal of the MG and RB by the Cpt was studied between 20 and 50ºC at natural pH values and the initial dye concentration of 80 mg/L. The amounts of dyes removed increased slightly with increases in the temperatures of both MG and RB solutions (Figure 6a,b). Increases in the removal of the dyes with increasing temperature may be attributed to the increasing thermal movement of dye molecules. A similar result was also reported for the adsorption of MG onto activated carbon prepared from Tunçbilek lignite (Önal *et al.*, 2006).

Removal of dyes in a two-dye system

For competitive removal of MG and RB in a two-dye system, the experiments were conducted separately using an initial concentration of 80 mg/L of each dye at natural dye pH values and at 20ºC in both systems. In a two-dye system, the pH values of the mixture were measured at between 3.91 and 3.94 and the degree of removal of both dyes decreased due to competitive adsorption (Figure 7). For example, the maximum extents of removal of MG and RB were 21.41 and 27.39 mg/g in a two-dye system while values of 36.75 and 34.90 mg/g, respectively, were found for single-dye systems. In a two-dye system, the removal of MG and RB decreased by ~41.74% and 21.51%, respectively, relative to single-dye systems. Similar results were reported for the competitive adsorption of reactive black onto filtrasorb 400 activated carbon in a multi-solute system (Al-Degs *et al.*, 2007) and of methylene blue and rhodamine B onto AlMCM-41 (Eftekhari *et al.*, 2010).

A mixture of binary or multi-solute systems can exhibit three possible types of adsorption behavior: synergism, antagonism, or non-interaction (Gao *et al.*, 2010; Li *et al.*, 2011; Wang *et al.*, 2012; Hernandez-Montoya *et al.*, 2013). Synergism indicates that the adsorption of the adsorbates in the mixture is greater than the adsorption of the individual adsorbate molecule in a single-dye system. Antagonism is where the adsorption of the adsorbates in the mixture is less than
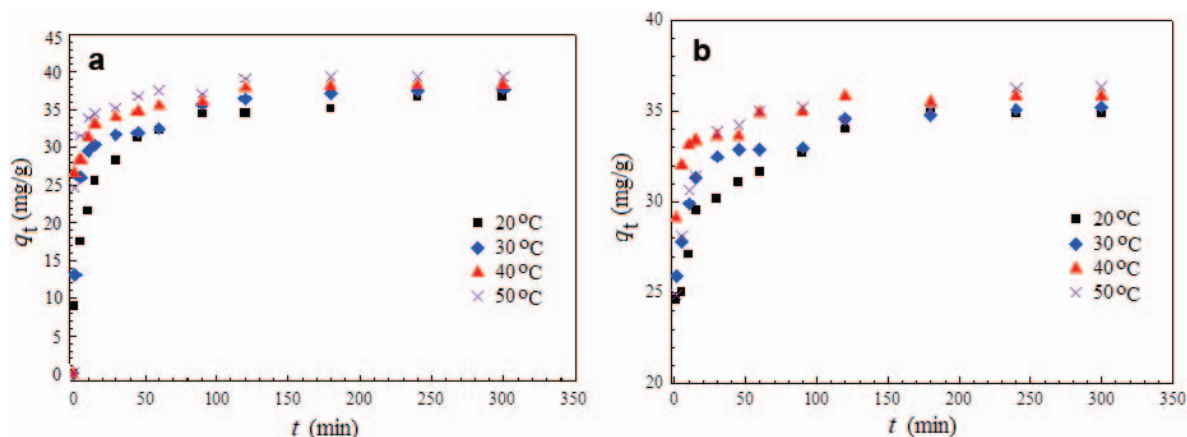

Figure 6. Effect of temperature on the adsorption of MG (a) and RB (b) dyes onto Cpt in a 2 g/L suspension at natural pH and 80 mg/L initial dye concentration.
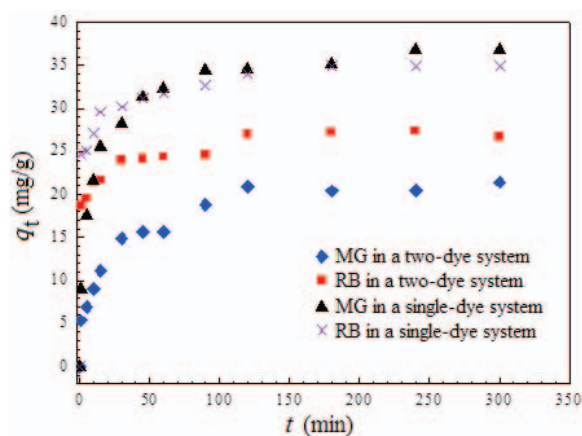
Figure 7. Adsorption of MG and RB in single- and two-dye systems in a 2 g/L suspension at 20ºC, natural pH, and 80 mg/L initial dye concentration.

the adsorption of the individual adsorbate molecules in a single-dye system. Non-interaction indicates that the adsorption of each of the adsorbate molecules in the mixture is almost unchanged relative to the adsorption of each dye in a single-dye system. In these experiments, the adsorption process showed an antagonistic effect. This effect points to a competition between MG and RB for the same exchange sites of the Cpt. As a result of this effect, the amount of each dye adsorbed decreased due to competitive adsorption in the two-dye system.

For a two-dye system, total removal efficiencies (*TRE*) of MG and RB by Cpt are shown in Figure 8a,b. When the initial concentration of MG increased from 20 to 100 mg/L for a constant concentration of 50 mg/L of the RB, the *TRE* decreased from 95.22 to 46.79%. Similarly, when the initial concentration of the RB increased from 20 to 100 mg/L for a constant concentration of 50 mg/L of the MB, its *TRE* decreased from 97.84 to 58.24%.
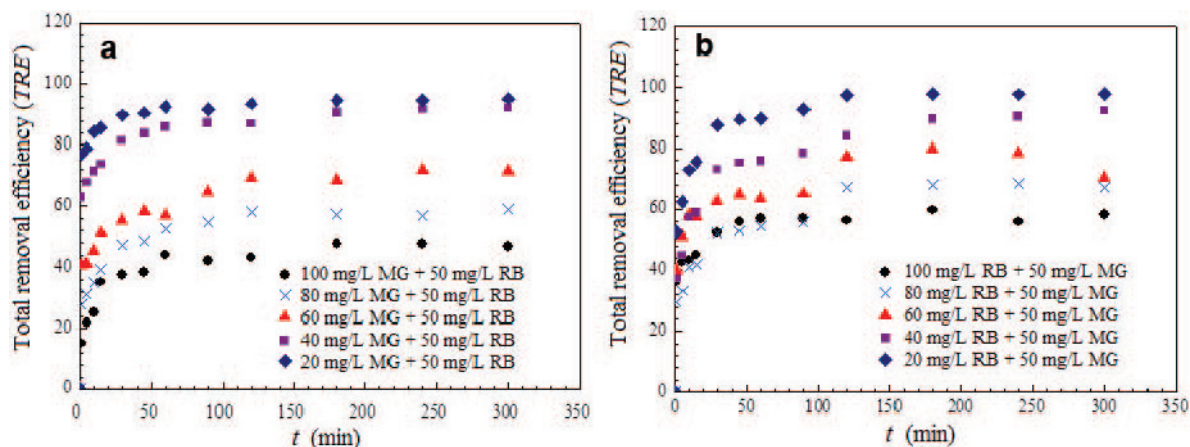
Relative adsorption and adsorption selectivity in a two-dye system

The relative adsorption of MG and RB in a two-dye system can be determined using equation 16 (Wang and Ariyanto, 2007):

$$A_{\mathrm{T}} = \frac{[q_{\mathrm{t}}]_{\mathrm{B}}}{[q_{\mathrm{t}}]_{\mathrm{S}}} \qquad (16)$$

where $[q_{\mathrm{t}}]_{\mathrm{S}}$ and $[q_{\mathrm{t}}]_{\mathrm{B}}$ are the amounts of MG and RB removed in both single- and two-dye systems at time *t*, respectively. Adsorption selectivity in a two-dye system can be estimated using equation 17 (Wang and Ariyanto, 2007):

$$S = \frac{(A_{\mathrm{r}})_{\mathrm{RB}}}{(A_{\mathrm{r}})_{\mathrm{MG}}} \qquad (17)$$

where *S* is the adsorption selectivity, and $(A_{\mathrm{r}})_{\mathrm{RB}}$ and $(A_{\mathrm{r}})_{\mathrm{MG}}$ are the relative adsorption of the RB and MG, respectively. In a two-dye system, the variation of the relative adsorption of MG and RB and the adsorption selectivity were determined (Figure 9). To determine the relative adsorption of the dyes, the initial concentration of each dye was selected as 80 mg/L in both systems. The change in relative adsorption of the RB may be negligible with increasing time (Figure 9). The relative adsorption of MG increased gradually with increase in time until a specific time (~120 min), and thereafter the relative adsorption of MG did not change significantly. The selectivity of adsorption, however, decreased and approached a constant value of 1.3 after an equilibrium time of 300 min. This situation indicated that the Cpt had a greater affinity for RB adsorption at the initial stage of adsorption in a two-dye system. Similar behavior was reported for the competitive adsorption of MG and Pb^{2+} ions on natural zeolite (Wang and Ariyanto, 2007), for competitive biosorption of yellow 2G and reactive brilliant red K-2G onto inactive aerobic granules (Gao *et al.*, 2010), and for competitive biosorption of acid blue 25 and acid red 337 onto unmodified and

Figure 8. Total removal efficiency of MG (a) and RB (b) dyes onto Cpt in a 2 g/L suspension in a two-dye system at 20ºC and natural pH (initial dye concentration of MG and RB in single- and two-dye systems: 80 mg/L, constant concentration of each dye in a two-dye system: 50 mg/L).
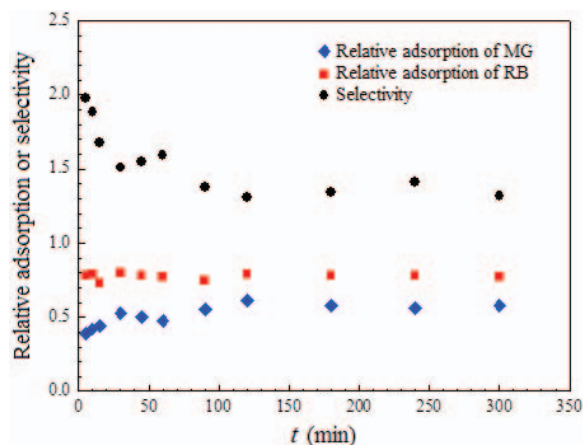
Figure 9. Relative adsorption and adsorption selectivity of MG and RB dyes onto Cpt in a 2 g/L suspension in a two-dye system at 20ºC and natural pH.

cetyldimethylethyl ammonium bromide-modified biomass of *Aspergillus oryzae* (Yang *et al.*, 2011).

Study of adsorption isotherms in single- and two-dye systems

The experimental equilibrium data for the adsorption of MG and RB onto Cpt were fitted to four isotherm models mentioned above in single- and two-dye systems. In a single-dye system, the experimental equilibrium data were determined for the initial dye concentrations of between 20 and 100 mg/L for MG, and between 60 and 120 mg/L for the RB at the natural pH values of the dyes and 20ºC, respectively. In a two-dye system, the experimental equilibrium data were calculated for the initial dye concentrations of 20−100 mg/L for MG or the RB at a constant initial concentration of 50 mg/L for each dye, respectively.

The values of Q_o and b were taken from the slope and the intercept, respectively, of the plot of C_e/q_e *vs.* C_e for the Langmuir-1 isotherm; the values of b and Q_o were taken from the slope and the intercept, respectively, of the plot of C_e/q_e *vs.* $1/C_e$ for the Langmuir-2 isotherm; the values of b and Q_o were taken from the slope and the intercept, respectively, of the plot of q_e/C_e *vs.* q_e for the Langmuir-3 isotherm; the values of n and k were taken from the slope and the intercept, respectively, of the plot of $\ln q_e$ *vs.* $\ln C_e$ for the Freundlich isotherm; the values of B and A_T were taken from the slope and the intercept, respectively, of the plot of q_e *vs.* $\ln C_e$ for the Temkin isotherm. The Redlich-Peterson isotherm contains three unknown constant parameters. In order to determine the constants of the Redlich-Peterson isotherm, a minimization procedure was applied using the 'solver add-in function' of Microsoft's *Excel*® program. Values of the constant K_R were determined by trying to maximize the values of the correlation coefficient (r^2) between the predicted values of q_e and the experimental data and to obtain a β value of <1. After determining the values of

K_R, the values of β and a_R were calculated from the slope and the intercept, respectively, of the linear plot of ln [K_R (C_e/q_e) − 1] *vs.* $\ln C_e$. All constant values of the Langmuir isotherm (Table 4) and the other isotherm constants (Table 5) were determined.

The adsorption of MG and RB matched the Langmuir-1 type isotherm best with r^2 values of between 0.987 and 1 for the MG and RB between the three Langmuir-type isotherms in single- and two-dye systems. When the values of the Langmuir-1 isotherm constant (Q_o) for the adsorption of MG and RB were 43.86 and 44.25 mg/g in a single-dye system, the values were 20.62 and 31.54 mg/g in a two-dye system, respectively. The values of Q_o determined for the adsorption of both dyes in a two-dye system were smaller because of competitive removal or adsorption. Compliance with the Langmuir-1 isotherm model indicates monolayer coverage of the dyes on the surface of the Cpt. Similar results were reported for the competitive adsorption of MB and RB on AlMCM-41 (Eftekhari *et al.*, 2010) and for binary adsorption of direct blue 78 and direct red 31 on activated carbon (Mahmoodi *et al.*, 2011) in single- and two-dye systems.

The values of the Freundlich constant (k) for the adsorption of MG and RB were 25.27 and 24.89 mg$^{1-1/n}$g^{-1} L$^{1/n}$ in a single-dye system; while values of 12.87 and 11.36 mg$^{1-1/n}$g^{-1} L$^{1/n}$ were found for a two-dye system. The values of k estimated for the adsorption of both dyes in a two-dye system were smaller due to competitive adsorption. The values of r^2 determined for the adsorption of MG and RB were between 0.898 and 0.988 in single- and two-dye systems (except for the adsorption of MG in a two-dye system). The higher values of r^2 in the Freundlich isotherm indicate reversible adsorption on a heterogeneous surface. A similar result was also reported for the adsorption of direct blue 78 and direct red 31 onto activated carbon in single- and two-dye systems (Mahmoodi *et al.*, 2011).

While the values of B related to the heat of adsorption from the Temkin equation were 5.78 and 5.07 J/mol for the adsorption of MG and RB in a single-dye system, the values were 2.06 and 4.83 J/mol, respectively, in the two-dye system. The values of B in the two-dye system were smaller than those in the single-dye system because of competitive adsorption. The values of r^2 from the Temkin equation for the adsorption of MG and RB were between 0.924 and 0.988 (except for the adsorption of MG in a two-dye system) in single- and two-dye systems. These values of r^2 showed that the adsorption isotherm obeyed the Temkin model in both systems. The compliance of the Temkin model of adsorption indicates a decrease in heat of adsorption with increasing coverage of the dyes on the surface of the Cpt. A similar result was reported for binary adsorption of direct blue 78 and direct red 31 onto activated carbon (Mahmoodi *et al.*, 2011).

Table 4. Langmuir isotherm parameters of the adsorption of MG and RB onto Cpt in single- and two-dye systems at 20°C.

System	Dye	Langmuir-1				Langmuir-2				Langmuir-3			
		Q_o (mg/g)	b (L/mg)	r^2	S.E.	Q_o (mg/g)	b (L/mg)	r^2	S.E.	Q_o (mg/g)	b (L/mg)	r^2	S.E.
Single	MG	43.86	2.40	0.9909	0.094	38.17	6.89	0.9310	0.039	40.58	5.26	0.8180	3.214
	RB	44.25	0.43	0.9876	0.020	40.98	0.89	0.8907	0.002	42.33	0.69	0.8058	2.506
Binary	MG	20.62	6.38	0.9985	0.097	22.27	1.24	0.9489	0.006	22.39	1.22	0.8124	3.266
	RB	31.54	0.32	0.9884	0.024	26.38	0.88	0.9698	0.006	28.18	0.69	0.8582	2.614

Table 5. Isotherm parameters of the adsorption of the MG and RB onto Cpt in single- and two-dye systems at 20°C.

System	Dye	Freundlich				Temkin					Redlich-Peterson				
		n (L/g)	k (mg$^{1-1/n}$g^{-1} L$^{1/n}$)	r^2	S.E.	A_T (L/g)	b_T	B (J mol^{-1})	r^2	S.E.	K_R (L/g)	a_R (L/mg)	β	r^2	S.E.
Single	MG	4.11	25.27	0.8979	0.013	136.30	421.29	5.7822	0.9734	0.182	440	14.59	0.85	0.9935	2.534
	RB	6.88	24.89	0.9506	0.043	102.85	480.18	5.0731	0.9245	0.050	176	6.51	0.88	0.9984	2.039
Binary	MG	7.18	12.87	0.6645	0.054	733.42	1179.95	2.0645	0.6978	0.109	31.30	1.45	0.99	0.9951	3.059
	RB	3.70	11.36	0.9885	0.063	10.58	503.98	4.8335	0.9880	0.031	73.40	5.40	0.78	0.9996	1.023

S.E. = Standard errors in estimates (from Alves and Lavorenti, 2004).

Table 6. Kinetic parameters of the adsorption of RB and MG onto the Cpt in single- and two-dye systems at 20°C.

System	Dye	C_0 (mg/L)	$q_{e\,(exp)}$ (mg/g)	Pseudo-first order model			Pseudo-second order model			Intra-particle diffusion					
				k_1 (min^{-1})	q_1 (mg/g)	r^2	k_2 (g/mg min)	q_2 (mg/g)	r^2	k_{i1} (mg/g min^2)	C_{i1}	r_1^2	k_{i2} (mg/g min^2)	C_{i2}	r_2^2
Single															
	MG	20	9.98	0.395	0.43	0.9587	2.863	9.99	1	0.126	9.553	0.7879	–	–	–
		40	19.93	0.109	2.37	0.9060	0.401	19.88	1	1.385	14.845	0.8899	0.001	19.867	0.0128
		60	29.62	0.062	8.56	0.9541	0.036	29.67	1	2.679	15.731	0.8227	0.020	29.228	0.2574
		80	36.75	0.011	13.26	0.7692	0.004	36.76	0.9990	3.732	8.223	0.9253	0.433	29.599	0.8998
		100	43.99	0.017	30.65	0.9436	0.001	46.73	0.9966	3.787	4.247	0.9091	0.588	34.237	0.7075
	RB	20	10.00	0.162	0.09	0.9528	3.571	10.00	1	0.029	9.890	0.9594	–	–	–
		40	19.99	0.063	0.12	0.9762	0.320	20.00	1	0.016	19.870	0.9906	0.001	19.980	0.4027
		60	28.85	0.013	3.37	0.9618	0.018	28.90	0.9999	0.565	23.842	0.9605	0.139	26.524	0.9796
		80	35.96	0.103	5.36	0.8394	0.014	35.46	0.9995	0.894	27.602	0.9400	0.144	32.944	0.5562
		100	39.13	0.028	7.55	0.8285	0.017	38.91	0.9996	0.598	32.471	0.9757	0.170	36.180	0.3827
Binary															
	MG	20	9.67	0.011	0.49	0.7017	0.145	9.66	1	0.287	8.228	0.9939	0.021	9.314	0.7712
		40	18.96	0.018	5.37	0.9630	0.013	19.12	0.9995	0.941	11.467	0.9931	0.188	15.950	0.9399
		60	20.46	0.017	5.76	0.8458	0.004	21.14	0.9965	1.436	6.009	0.7985	0.577	11.516	0.8648
		80	21.41	0.013	11.38	0.7800	0.003	22.03	0.9967	1.999	2.971	0.9633	0.570	12.359	0.8089
		100	20.22	0.028	20.76	0.9089	0.002	21.69	0.9968	3.870	-4.389	0.9225	0.556	11.528	0.8325
	RB	20	9.69	0.025	3.13	0.9192	0.027	9.79	0.9996	0.472	5.855	0.9801	0.099	8.175	0.8426
		40	17.98	0.014	5.62	0.8638	0.009	18.18	0.9987	0.986	9.605	0.9570	0.285	13.449	0.8518
		60	23.33	0.017	5.76	0.8458	0.012	23.42	0.9992	1.163	15.427	0.8997	0.280	18.869	0.8221
		80	27.39	0.022	8.65	0.9261	0.009	27.39	0.9990	1.108	17.472	0.9392	0.313	22.309	0.7646
		100	31.26	0.017	4.24	0.8947	0.146	30.21	0.9987	0.686	25.209	0.8900	0.061	29.489	0.1499

The values of r^2 determined from the R-P model were between 0.9935 and 0.9996 for the adsorption of MG and RB in single- and two-dye systems, and the values of β were ~1 (Table 5). These results indicated the applicability of the R-P model. Similar results were also reported for the competitive adsorption of remazol reactive yellow, remazol reactive black, and remazol reactive red onto filtrasorb 400 activated carbon (FS400) in single- and two-dye systems (Al-Degs *et al*., 2007). The results of the isotherm studies showed that the adsorption of MG and RB followed the mathematical relationships given by the Langmuir, Freundlich, Temkin, and R-P isotherms.

Study of adsorption kinetics in single- and two-dye systems

In single- and two-dye systems, the process of adsorbing MG and RB onto the Cpt was studied using the three kinetics models (pseudo-first order, pseudo-second order, and intra-particle diffusion) mentioned above. The adsorption kinetics of MG and RB onto Cpt were studied for initial concentrations of 20 to 100 mg/L at natural dye pH values and 20ºC according to the three models. The values of q_1 and k_1 from the slope and intercept of the linear plots of $\log(q_e - q_t)$ *vs*. t for the pseudo-first order model; the values of q_2 and k_2 from the slope and the intercept of the linear plots of t/q_t *vs*. t for the pseudo-second order model; the values of k_i and C from the slope and the intercept of the linear plots of q_t *vs*. $t^{1/2}$ for the intra-particle diffusion model were calculated. All of the kinetics parameters were estimated from the models above (Table 6). In single- and two-dye systems, the values of correlation coefficients (r^2) from the pseudo-first order kinetics model were between 0.7017 and 0.9762 for the adsorption of MG and RB. The values of q_1 from the pseudo-first order kinetics model did not agree with the experimental data, $q_{e(exp.)}$, although values of r^2 were large. This indicates that the adsorption process did not obey the pseudo-first order kinetics model. Graphs for pseudo-first order kinetics, therefore, are not shown.

The kinetics parameters such as correlation coefficients (r^2), theoretical adsorption capacities (q_2), and adsorption-rate constants (k_2) were determined from the regression analyses of linear plots of t/q_t *vs*. t for the pseudo-second order kinetics in single- and two-dye systems (Table 6). The values of r^2 from the pseudo-second order kinetics model were 0.9965 and 1.00 for the adsorption of MG and RB in single- and two-dye systems (see Table 5). The values of q_2 were consistent with the experimental data, $q_{e(exp)}$, and the adsorption of both dyes, therefore, obeyed the pseudo-second order kinetics model, indicating chemical activation between the Cpt and dye molecules. Similar results were reported for the competitive adsorption of methylene blue and rhodamine B onto AlMCM-41 (Eftekhari *et al*., 2010) and for binary adsorption of direct blue 78 and direct red

31 onto activated carbon (Mahmoodi *et al*., 2011). The rate constants, k_2, in a two-dye system were smaller than those of a single-dye system because of competitive adsorption of dye molecules in a two-dye system.

The plots of q_t *vs*. $t^{1/2}$ for the intra-particle diffusion model in both systems comprised two phases. Phase I represented migration from the bulk phase to the adsorbent surface, and phase II accounted for intra-particle diffusion of the adsorbate into the particles. The intra-particle diffusion rate constants (k_{i1} and k_{i2}), the correlation coefficients (r_1^2 and r_2^2), and the thickness of the boundary layer (values C_{i1} and C_{i2}) for phases I and II were obtained (Table 6). The values of r_1^2 and k_{i1} for the adsorption of MG and RB for phase I were greater than those of phase II in single- and two-dye systems. The values of the C_{i1} and C_{i2} from the intercept of the intra-particle diffusion equation increased with increasing initial dye concentration for the adsorption of MG and RB in both systems (except for the values C_{i1} of MG adsorption in both systems). The results showed that the adsorption process did not obey intra-particle diffusion. The large r_1^2 values for phase I indicated migration from the bulk phase to the external surface of the Cpt.

CONCLUSIONS

Clinoptilolite may be used as an effective and selective adsorbent for the removal of MG and RB from single- and two-dye systems. In a two-dye system, the clinoptilolite had greater affinity for RB and it was, therefore, adsorbed selectively relative to the MG, and the adsorption of MG and RB decreased by ~41.74% and 21.51% due to competitive adsorption, respectively. In single- and two-dye systems, the adsorption of MG and RB indicated monolayer coverage on the surface of the clinoptilolite. Kinetics studies showed that chemical activation may occur between the clinoptilolite and the dyes.

REFERENCES

Acemioğlu, B. (2004) Adsorption of Congo red from aqueous solution onto calcium-rich fly ash. *Journal of Colloid and Interface Science* **274**, 371−379.

Acemioğlu, B., Kertmen, M., Digrak, M., and Alma, M.H. (2010) Use of *Aspergillus wentii* for biosorption of methylene blue from aqueous solution. *African Journal of Biotechnology*, **9**, 874−881.

Al-Degs, Y., Khraisheh, M.A.M., Allen, S.J., Ahmad, M.N., and Walker, G.M. (2007) Competitive adsorption of reactive dyes from solution: Equilibrium isotherm studies in single and multisolute systems. *Chemical Engineering Journal*, **128**, 163−167.

Alpat, S.K., Ozbayrak, O., Alpat, S., and Akcay, H. (2008) The adsorption kinetics and removal of cationic dye. Toluidine

blue O from aqueous solution with Turkish zeolite. *Journal of Hazardous Materials*, **151**, 213–220.

Alvarez-Ayuso, E., Garcia-Sanchez, A., and Querol, X. (2003) Purification of metal electroplating waste waters using zeolites. *Water Research*, **37**, 4855–4862.

Alves, M.E. and Lavorenti, A. (2004) Sulfate adsorption and its relationships with properties of representative soil of the São Paulo State, Brazil. *Geoderma*, **118**, 89–99.

Anandkumar, J. and Mandal, B. (2011) Adsorption of chromium(VI) and Rhodamine B by surface modified tannery waste: Kinetic, mechanistic and thermodynamic studies. *Journal of Hazardous Materials*, **186**, 1088–1096.

Armagan, B., Turan, M., and Celik, M.S. (2004) Equilibrium studies on the adsorption of reactive azo dyes into zeolite. *Desalination*, **170**, 33–39.

Benkli, Y.E., Can, M.F., Turan, M., and Celik, M.S. (2005) Modification of organo-zeolite surface for the removal of reactive azo dyes in fixed-bed reactors. *Water Research*, **39**, 487–493.

Bilir, M.H., Sakalar, N., Acemioğlu, B., Baran, E., and Alma, M.H. (2013) Sorption of remazol brilliant blue R onto polyurethane-type foam prepared from peanut shell. *Journal of Applied Polymer Science*, **6**, 4340–4351.

Chen, C.Y., Chang, J.C., and Chen, A.H. (2011) Competitive biosorption of azo dyes from aqueous solution on the templated crosslinked-chitosan nanoparticles. *Journal of Hazardous Materials*, **185**, 430–441.

Chowdhury, S., Mishra, R., Saha, P., and Kushwaha, P. (2011) Adsorption thermodynamics, kinetics and isosteric heat of adsorption of malachite green onto chemically modified rice husk. *Desalination*, **265**, 159–168.

Dawood, S. and Sen, T.K. (2012) Removal of anionic dye Congo red from aqueous solution by raw pine and acid-treated pine cone powder as adsorbent: Equilibrium, thermodynamic, kinetics, mechanism and process design. *Water Research*, **46**, 1933–1946.

Dogan, M. and Alkan, M. (2003) Adsorption kinetics of methyl violet onto perlite. *Chemosphere* **50**, 517–528.

Eftekhari, S., Habibi-Yangjeh, A., and Sohrabnezhad, Sh. (2010) Application of AlMCM-41 for competitive adsorption of methylene blue and rhodamine B: Thermodynamic and kinetic studies. *Journal of Hazardous Materials*, **178**, 349–355.

Ertaş, M., Acemioğlu, B., Alma, M.H., and Usta, S. (2010) Removal of methylene blue from aqueous solution using cotton stalk, cotton waste and cotton dust. *Journal of Hazardous Materials*, **183**, 421–427.

Farhadi, K., Matin, A.A., and Hashemi, P. (2010) Removal of malachite green from aqueous solutions using molecularly imprinted polymer. *Desalination and Water Treatment*, **24**, 20–27.

Farmer, V.C. (editor) (1974) *The Infrared Spectra of Minerals*. Mineralogical Society, London.

Freundlich, H.M.F. (1906) Über die adsorption in lösungen. *Zeitschrift für Physikalische Chemie*, **57A**, 385–470.

Gao, J.F., Zhang, Q., Su, K., and Wang, J.H. (2010) Competitive biosorption of yellow 2G and reactive brilliant red K-2G onto inactive aerobic granules: Simultaneous determination of two dyes by first-order derivative spectrophotometry and isotherm studies. *Bioresource Technology*, **101**, 5793–5801.

George, J.M. (1982) *Microscopic Aspects of Adhesion and Lubrication*. Tribology series, **7**. Elsevier Scientific Publishing Company, Amsterdam.

Guo, Y., Zhao, J., Zhang, H., Yang, S., Qi, J., Wang, Z., and Xu, H. (2005) Use of rice husk-based porous carbon for adsorption of rhodamine B from aqueous solutions. *Dyes and Pigments*, **66**, 123–128

Hameed, B.H. and El-Khaiary, M.I. (2008a) Batch removal of malachite green from aqueous solutions by adsorption on oil

palm trunk fibre: Equilibrium isotherms and kinetic studies. *Journal of Hazardous Materials*, **154**, 237–244.

Hameed, B.H. and El-Khaiary, M.I. (2008b) Kinetics and equilibrium studies of malachite green adsorption on rice straw-derived char. *Journal of Hazardous Materials*, **153**, 701–708.

Han, R., Wang, Y., Sun, Q., Wang, L., Song, J., He, X., and Dou, C. (2010) Malachite green adsorption onto natural zeolite and reuse by microwave irridation. *Journal of Hazardous Materials* **175**, 1056–1061.

Hernandez-Montoya, V., Perez-Cruz, M.A., Mendoza-Castillo, D.I., Moreno-Virgen, M.R., and Bonilla-Petriciolet, A. (2013) Competitive adsorption of dyes and heavy metals on zeolitic structures. *Journal of Environmental Management*, **116**, 213–221.

Hisarli, G., Tezcan, C., and Atun, G. (2012) Adsorption kinetics and equilibria of basic dyes onto zeolite in single and binary systems. *Chemical Engineering Communication*, **199**, 1412–1436.

Ho, Y.S. and McKay, G. (1998) Sorption of dye from aqueous solution by peat. *Chemical Engineering Journal*, **70**, 115–124.

Lagergren, S. (1898) About the theory of so-called adsorption of soluble substance. *Kungliga Svenska Vetenskapsakademiens. Handlingar. Band*, **24**, 1–39.

Langmuir, I. (1918) The adsorption of gases on plane surfaces of glass, mica and platinum. *Journal of American Chemical Society*, **40**, 1361–1403.

Li, L., Liu, F., Jing, X., Ling, P., and Li, A. (2011) Displacement mechanism of binary competitive adsorption for aqueous divalent metal ions onto a novel IDA-chelating resin: Isotherm and kinetic modeling. *Water Research*, **45**, 1177–1188.

Mahmoodi, N.M., Salehi, R., and Arami, M. (2011) Binary system dye removal from colored textile wastewater using activated carbon: Kinetic and isotherm studies. *Desalination* **272**, 187–195.

Maleki, R., Farhadi, K., and Nikkhahi, Y. (2012) Trace determination of malachite green in water samples using dispersive liquidliquid microextraction coupled with high-performance liquid chromatography-diode array detection. *International Journal of Environmental Analytical Chemistry*, **92**, 1026–1035.

Margeta, K., Zabukovec Logar, N., Šiljeg, M., and Farkaš, A. (2013) Natural zeolites in water treatment – how effective is their use? Pp. 81–112 in: *Water Treatment* (W. Elshorbagy, editor). InTech, DOI: 10.5772/50738. Available from: http://www.intechopen.com/.

Milanova, D., Chambers, R.D., Bahga, S.S., and Santiago, J.G. (2012) Effect of PVP on the electroosmotic mobility of wet-etched glass microchannels. *Electrophoresis*, **33**, 3259–3262.

Ming, D.W. and Dixon, J.B. (1987) Quantitative determinatıon of clinoptilolite in soils by a cation-exchange capacity method. *Clays and Clay Minerals* **35**, 463–468.

Nandi, B.K., Goswami, A., and Purkait, M.K. (2009) Adsorption characteristics of brilliant green dye on kaolin. *Journal of Hazardous Materials*, **161**, 387–395.

Ofomaja, A.E. and Ho, Y.S. (2008) Effect of temperatures and pH on methyl violet biosorption by mansonia wood sawdust. *Bioresource Technology*, **99**, 5411–5417.

Önal, Y., Akmil-Başar, C., Eren, D., Sarıcı-Özdemir, C., and Depci, T. (2006) Adsorption kinetics of malachite green onto activated carbon prepared from Tuncbilek lignite. *Journal of Hazardous Materials*, **B128**, 150–157.

Öncel, M., Güvenç, İ., and Acemioğlu, B. (2012) Use of pirina pretreated with hydrochloric acid for the adsorption of methyl violet from aqueous solution. *Asian Journal of Chemistry* **24**, 1698–1704.

Özdemir, A. and Kekin, C.S. (2009) Removal of a binary dye mixture of Congo red and malachite green from aqueous solutions usıng a bentonite adsorbent. *Clays and Clay Minerals*, **57**, 695−705.

Özdemir, M., Bolgaz, T., Saka, C., and Şahin, Ö. (2011) Preparation and characterization of activated carbon from cotton stalks in a two-stage process. *Journal of Analytical and Applied Pyrolysis*, **92**, 171−175.

Redlich, O. and Peterson, D.L. (1959) A useful adsorption isotherm. *Journal of Physical Chemistry*, **63**, 1024−1026.

Samil, A., Acemioğlu, B., Gültekin, G., and Alma, M.H. (2011) Removal of remazol orange RGB from aqueous solution by peanut shell. *Asian Journal of Chemistry*, **23**, 3224−3230.

Sismanoglu, T., Kismir, Y., and Karakus, S. (2010) Single and binary adsorption of reactive dyes from aqueous solutions onto clinoptilolite. *Journal of Hazardous Materials*, **184**, 164−169.

Sprynskyy, M., Buszewski, B., Terzyk, A.P., and Namiesnik, J. (2006) Study of the selection mechanism of heavy metal (Pb^{2+}, Cu^{2+}, Ni^{2+}, and Cd^{2+}) adsorption on clinoptilolite. *Journal of Colloid and Interface Science*, **304**, 21−28.

Tarlan-Yel, E. and Önen, V. (2010) Performance of natural zeolite and sepiolite in the removal of free cyanide and copper-complexed cyanide ($[Cu(CN)_3]^{2-}$). *Clays and Clay Minerals*, **58**, 110−119.

Temkin, M.J. and Pyzhev, V. (1940) Kinetics of ammonia synthesis on promoted iron catalysts. *Acta Physiochim URSS*, **12**, 327−356.

Tomić, S., Rajić, N., Hrenović, J., and Povrenović, D. (2012) Removal of Mg from spring water using natural clinoptilolite. *Clay Minerals*, **47**, 81−92.

Uğurlu, M. (2009) Adsorption of a textile dye onto activated sepiolite. *Microporous and Mesoporous Materials* **119**, 276−283.

Uğurlu, M., Gürses, A., and Açıkyıldız, M. (2008) Comparison of textile dyeing effluent adsorption on commercial activated carbon and activated carbon prepared from olive stone by $ZnCl_2$ activation. *Microporous and Mesoporous Materials* **111**, 228−235.

Vala, R.M.K. and Tichagwa, L., (2013) Enhancement of the adsorption of phenol red from wastewater onto clinoptilolite by modificatıon wıth n-terminated siloxanes. *Clays and Clay Minerals*, **61**, 532−540.

Wang, S. and Ariyanto, E. (2007) Competitive adsorption of malachite green and Pb^{2+} ions on natural zeolite. *Journal of Colloid and Interface Science*, **314**, 25−31.

Wang, S. and Peng, Y. (2010) Natural zeolites as effective adsorbents in water and wastewater treatment. *Chemical Engineering Journal*, **156**, 11−24.

Wang, S., Ng, C.W., Wang, W., Li, Q., and Hao, Z. (2012) Synergistic and competitive adsorption of organic dyes on multiwalled carbon nanotubes. *Chemical Engineering Journal*, **197**, 34−40.

Wang, S.B. and Zhu, Z.H. (2006) Characterisation and environmental application of an Australian natural zeolite for basic dye removal from aqueous solution. *Journal of Hazardous Materials*, **B136**, 946−952.

Weber, W.J. and Morris, J.C. (1963) Kinetics of adsorption on carbon from solution. *Journal of Sanitary Engineering Division, ASCE*, **89(SA2)**, 31−39.

Won, S.W, Han, M.H., and Yun, Y.S. (2008) Different binding mechanism in biosorption of reactive dyes according to their reactivity. *Water Research* **42**, 4847−4855.

Yang, Y., Jin, D., Wang, G., Wang, S., Xiaoming Jia, J., and Zhao, Y. (2011) Competitive biosorption of acid blue 25 and acid red 337 onto unmodified and CDAB-modified biomass of *Aspergillus oryzae*. *Bioresource Technology*, **102**, 7429−7436.

Yazici, M., Acemioğlu, B., Akbas, M., and Kuvet, M. (2016) Determination of the ground and excited-state dipole moments of 4'-(Hexyloxy)-4-biphenylcarbonitrile and 4-Isothiocyanatophenyl 4-Pentylbicyclo [2,2,2]octane-1-carboxylate nematic liquid crystals and their mixtures. *Liquid Crystal*, **45**, 678−890.

Zhang, R., Hummelgård, M., Lv, G., and Olin, H. (2011) Real time monitoring of the drug release of rhodamine B on graphene oxide. *Carbon*, **49**, 1126−1132.

Zou, Y., Zhang, Z., Shao, X., Chen, Y., Wu, X., Yang, L., Zhu, J., and Zhang, D. (2014) Application of three-phase hollow fiber LPME using an ionic liquid as supported phase for preconcentration of malachite green from water samples with HPLC detection. *Bulletin of the Korean Chemical Society*, **35**, 371−376.